CLINICALLY RELEVANT

Nanomedicine: Nanotechnology, Biology, and Medicine
7 (2011) 497–504

Research Article

nanomedjournal.com

Modulation of collagen alignment by silver nanoparticles results in better mechanical properties in wound healing

Karen H.L. Kwan, BSc[a,1], Xuelai Liu, MD[b,1], Michael K.T. To, MBBS[a,1], Kelvin W.K. Yeung, PhD[a], Chi-ming Ho, PhD[c], Kenneth K.Y. Wong, MD, PhD[b,*]

[a]*Department of Orthopaedics and Traumatology, LKS Faculty of Medicine, University of Hong Kong, Hong Kong, China*
[b]*Department of Surgery, LKS Faculty of Medicine, University of Hong Kong, Hong Kong, China*
[c]*Department of Chemistry, University of Hong Kong, Hong Kong, China*

Received 10 September 2010; accepted 10 January 2011

Abstract

Our previous study has revealed that silver nanoparticles (AgNPs) have potential to promote wound healing by accelerated re-epithelization and enhanced differentiation of fibroblasts. However, the effect of AgNPs on the functionality of repaired skin is unknown. The aim of this study was to explore the tensile properties of healed skin after treatment with AgNPs. Immunohistochemical staining, quantitative assay and scanning electron microscopy (SEM) were used to detect and compare collagen deposition, and the morphology and distribution of collagen fibers. Our results showed that AgNPs improved tensile properties and led to better fibril alignments in repaired skin, with a close resemblance to normal skin. Based on our findings, we concluded that AgNPs were predominantly responsible for regulating deposition of collagen and their use resulted in excellent alignment in the wound healing process. The exact signaling pathway by which AgNPs affect collagen regeneration is yet to be investigated.

From the Clinical Editor: The aim of this study was to explore the tensile properties of healed skin after treatment with AgNPs. These nanoparticles improved tensile properties and led to better fibril alignments in repaired skin, with a close resemblance to normal skin. The exact signaling pathway by which AgNPs affect collagen regeneration is yet to be investigated.

Key words: Silver nanoparticles; Healing; Tensile strength; Collagen organization

Wound healing is a complicated process that is characterized by angiogenesis, granulation tissue formation, collagen deposition, epithelialization and wound contraction.[1,2] All these phases involve complex biomolecular interactions among soluble cytokines, formed blood elements, the extracellular matrix and cells.[2] Ideally, repaired skin should be cosmetically and functionally identical to normal skin, which requires that the repaired wound not only be restored to normal anatomical structures, but also that it reaches an acceptable level functionally. Collagen is the main element that furnishes connective tissues with mechanical integrity, and it plays an important role in load bearing. In skin, collagen is produced mainly by fibroblasts in the dermal layer, with collagen type I and type III being the most abundant.[3] Injuries that would lead to damage to the structure thus result in the loss of skin integrity. Hence, as a protection against external stimuli[2] and to provide a platform for re-epithelization, regeneration of collagen after injury is an essential process.[4] Furthermore, normal synthesis and distribution of collagen in skin will also contribute greatly to restoring skin functionality.

Our previous studies have already shown enhanced efficiency of healing by the application of silver nanoparticles (AgNPs) on skin wounds in both burn and excisional models in mice.[5,6] Macroscopic observation and histological examination further confirmed the remarkable resemblance of AgNP-treated skin to normal skin after healing. Because collagen organization is the foundation of skin's mechanical properties, a question has arisen as to whether the mechanical function of healed AgNP-treated skin is also similar to that of normal skin. Through in vitro and in vivo studies, we showed that AgNPs could inhibit the proliferation of fibroblasts and the production of collagen in the early phase of healing. Nonetheless, the characteristics of collagen in terms of the fibril network and organization in both the later phase of healing and after healing remain unknown.

Disclosures: The authors have no financial disclosures, and this work was supported by Seed Funding Programme for Basic Research, HKU (no. 200603159001).

*Corresponding author.
E-mail address: kkywong@hku.hk (K.K.Y. Wong).

[1] These authors contributed equally to this work.

1549-9634/$ – see front matter © 2011 Elsevier Inc. All rights reserved.
doi:10.1016/j.nano.2011.01.003

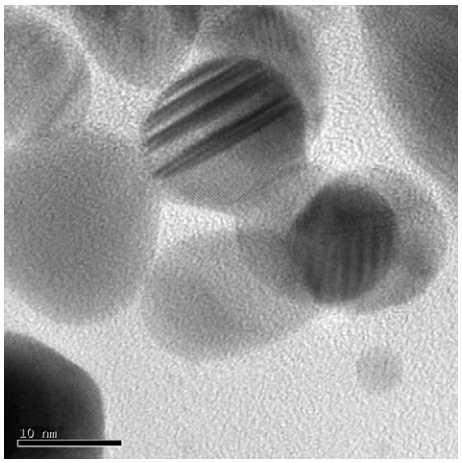

Figure 1. TEM picture showing the morphology and size (Diameter: 5–15 nm) of AgNPs used in this study.

Thus, the aim of this study was to explore the effect of AgNPs on collagen formation and deposition at the point of complete wound healing, as we hypothesized that AgNPs could modulate collagen deposition, which would be reflected in the improved mechanical properties of the regenerated skin.

Methods

Preparation of AgNPs

The synthesis of AgNPs has already been described.[6] The final concentration of solution was 1 mM. The mean diameter of AgNPs averaged 10 nm (and ranged from 5 to 15 nm), as confirmed by transmission electron microscopy (TEM) as shown in Figure 1.

Excisional wound model

In this study, 6- to 8-week-old C57BL/6N mice, weighing 18-22 grams were obtained from the Laboratory Animal Unit, The University of Hong Kong. The animals were allowed diet and water ad libitum in a room with alternating periods of 12 hours light and 12 hours dark. The experimental protocol was approved by the Committee of the Use of Live Animals in Teaching and Research, University of Hong Kong (CULATR 1974-09). Anesthesia for experimentation was achieved with an intraperitoneal injection of pentobarbital sodium solution (Abbott Laboratories, Hong Kong) at a dose of 50 mg/Kg.

Mice were randomly divided into three groups: a normal group, the AgNP group, and an untreated group (n = 5). A 2.0 × 2.0 cm^2 full-thickness excisional wound was created after anesthesia. A dressing coated with AgNP solution (dose: 0.04 mg/cm^2) was topically applied to the wound bed in AgNP group. The wound dressings were changed daily until the wound was healed. A simple sterile dressing was covered to wound bed in the untreated group. The criterion of complete wound healing was defined by the denuded wound surface being completely covered by layers of keratinocytes, and when a new stratified epidermis with underlying basal lamina was re-established from the margins of the wound.[7-9] Specimens in various groups were harvested as soon as the wounds completely healed.

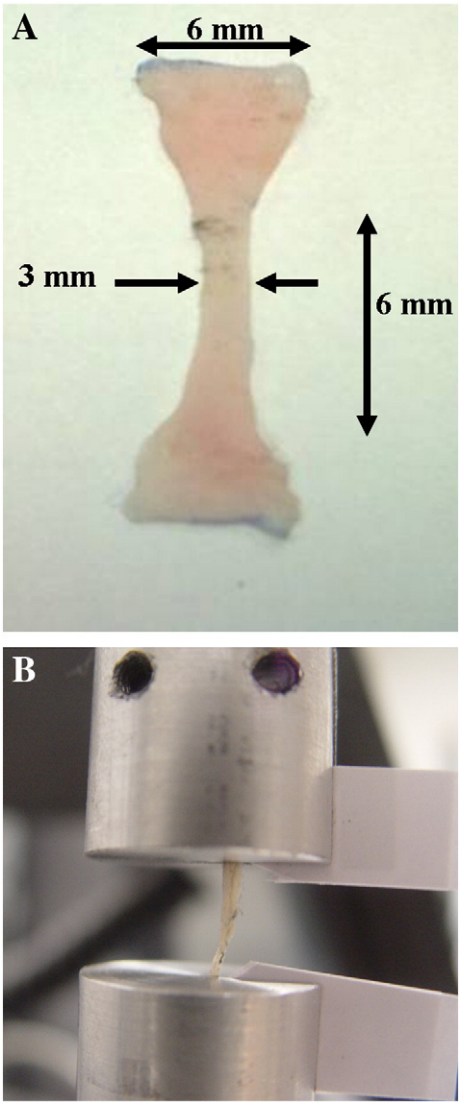

Figure 2. **(A)** Picture showing the dumbbell-shaped specimen taken from healed wound. The thickness of the sample was measured with the Venier Caliper before loading. The skin thickness ranged from 0.3 to 0.5 mm. **(B)** Specimens under applied tensile force at a rate of 1 mm/sec. The specimen was closely monitored during the test to ensure rip occurred within the gauge length, which was the region being exposed after loading.

Tensile tests

The tensile tests were conducted by researchers who were blind to the different treatment groups. The excised skin tissue was cut into a dumbbell shape with the aid of a custom-made metal template to ensure that breakage occurred at the gauge length (the region with reduced cross-sectional area where elongation was measured) instead of the gripped area during the tensile test. The overall test specimen was 20 mm in length and 6 mm in width; the mid part measured 3 mm in width and 6 mm in length (Figure 2, *A*). To ensure homogeneity of the specimens, all samples were excised in the same orientation relative to the mice anatomy along the anterior–posterior axis. Additionally, the thickness of skin and the width of the gauge region were

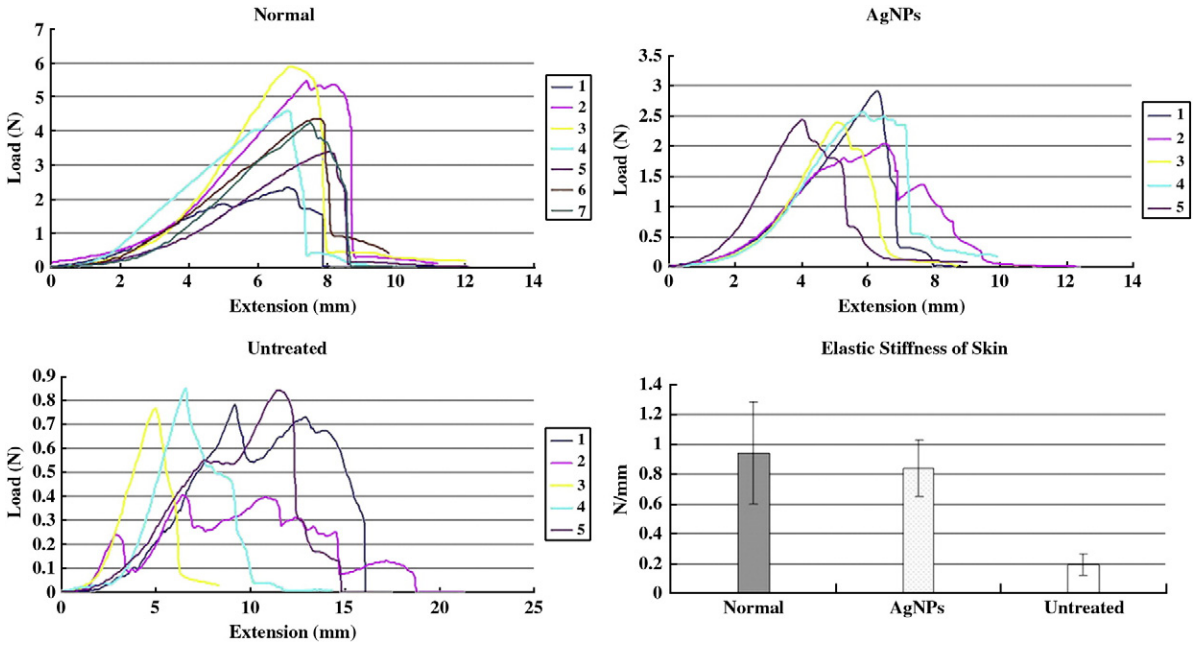

Figure 3. Force-displacement graphs for the normal, untreated and AgNP-treated groups. The force-displacement curve measured the tensile load applied on the sample as the grips attached to the load cell progressively moved apart.

measured with the Venier Caliper before loading. The tensile test was performed using the Instron 5848 MicroTester (Instron, Norwood, Massachusetts) with a 100N load cell at constant strain rate of 1 mm/sec (Figure 2, *B*). Specimens were loaded with the aid of a paper frame and held by the grips attached to the load cell. For the test, the tested skin was first stretched to its original dimension of 2 × 2 cm to mimic its natural state on the mice body before tensile-force application. The test ended when the sample was completely broken.

Masson trichrome staining and IHC

The healed skins were harvested, formalin-fixed and embedded in paraffin. Next, 5 μm sections were microtome sliced, de-waxed and rehydrated. Collagen fiber was stained using the Masson trichrome method. In brief, the rehydrated paraffined sections were mordant in preheated Bouin's solution at 56°C for 15 minutes. The slides were cooled and washed in tap water to remove the yellow coloring. The slides were stained in working Weigert's iron hematoxylin solution for 5 minutes and were then rinsed. , Next, the slides were stained with Biebrich scarlet-acid Fucshin solution, Phosphotungstic/Phosphomolybdic acid solution and Aniline Blue solution for 5 minutes in tandem with rinsing between each stain. The slides were then placed in acetic acid (1%) for 2 minutes, then rinsed, dehydrated by alcohol, cleared in xylene and finally mounted. Images were viewed under microscopy.

For immunostaining of collagen types I and III, healed skin tissues were harvested and processed as previously. Endogenous peroxidase was quenched by treatment in 3% hydrogen peroxide/methanol for 10 minutes. Sections were then incubated in a blocking solution containing 5% normal goat serum (Dako Bioreasearch, Canada). For antigen retrieval of collagen type I and type III, the sections were further blocked for nonspecific binding with 10% normal goat serum before anticollagen I primary antibody (rabbit-anti-mouse, Abcam, Cambridge, Massachusetts) (1:400) and anticollagen III primary antibody (rabbit-anti-mouse, Abcam) (1:100) was added respectively. The sections were incubated overnight at 4°C before being rinsed in PBS, and then incubated with HRP-conjugated secondary antibody (Santa Cruz Biotechnologies, Santa Cruz, California). Positive signals were developed by using DAB (3,3′-diaminobenzide tetrahydrochloride) and counterstained with hematoxylin. Images were viewed under microscopy.

Collagen content measurement

Medugorac's method was referred to detect hydroxyproline (Hyp) concentration in specimen.[2,10,11] Hyp kit was purchased from JianChen Gene Company (Nanjing, PR China) to detect the production of Hyp and content of collagen. The healed skin tissues (n = 5) were harvested and cut into pieces and then incubated with tissue lysis buffer for 10 minutes and homogenized. The tubes were centrifuged (13,000 rpm) at 4°C and supernatant was collected. Total protein concentration was evaluated by using protein assay kit according to the manufacturer's instructions (Bio-rad, Hercules, California). The average value was taken from triplicate readings. The ratio between collagen and total protein in specimen was calculated.

Scanning Electron Microscopy (SEM)

SEM was used as a tool for visualization and verification of the tensile test result. Skin tissues were fixed in 10% neutral buffered formalin for 2 hours at 4°C and washed well in several changes of cacodylate buffer with 0.1M sucrose to remove excess fixative. The tissues were then dehydrated in 30%, 50%,

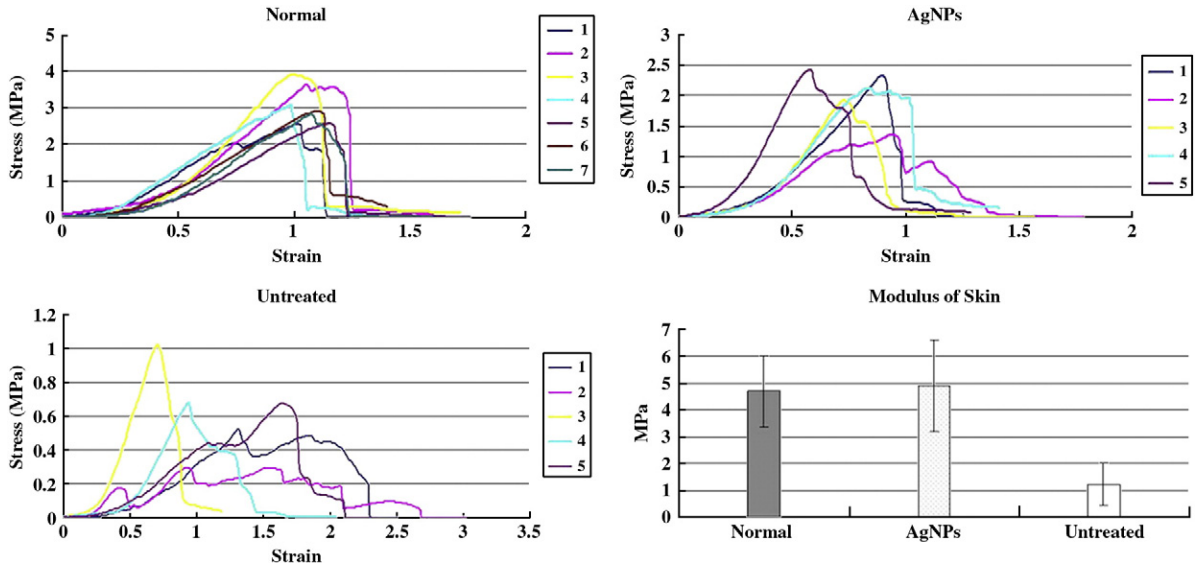

Figure 4. Graphs showing the stress-strain relationship of the tensile test. Dimensional variations were taken into account by normalization. Stress σ was calculated with the equation F/A, where F is the load and A is the cross-sectional area of the mid-point within the gauge length. Strain ε was computed as ΔL/L, where ΔL is the length of extension and L is the original gauge length.

70% and 90% ethanol in sequential order and finally dehydrated in 100% ethanol. The samples were then dried in a Critical Point Dryer and mounted on SEM specimen holders. A thin layer of metallic film was coated onto the specimen for 30 seconds as the last step of the preparation. Imaging was performed with Hitachi S4800 FEG SEM. Imaging was performed on samples of different groups before and after the tensile test to evaluate the architecture of the collagen fibril matrix and to observe the fracture pattern. The fibrils' size was measured with Image J (NIH, USA).

Statistic analysis

Statistical analyses were performed using Student's paired t-test. A p value of < 0.05 was considered significant. The results showed the average value ± standard deviation.

Results

AgNP-treated skin had mechanical properties similar to those of normal skin

We first used tensile tests to explore and compare the mechanical properties of the healed skins in the normal group, in the AgNP group and in the untreated group. Force-displacement graph showed the results of the yielding load and elastic stiffness (Figure 3). The yielding load was indicated by the plateau on the curve, which represented the failure point and thus the physical strength of the healed skin. The average yielding load for normal (n = 7), AgNP (n = 5) and untreated (n = 5) specimens was 4.25 ± 1.34N, 2.47 ± 0.31N and 0.64 ± 0.25N, respectively. The yielding load of the skin in AgNP group was significantly higher than that of untreated group ($p < 0.001$).

On the other hand, the linear gradient of the force-displacement graph represented elastic stiffness of the tissues. Results there showed that the average elastic stiffness for normal, AgNP-treated and untreated specimens was 0.94 ± 0.34 N/mm, 0.84 ± 0.19N/mm and 0.19 ± 0.07 N/mm, respectively (Figure 3). Indeed, no significant difference was found between the normal skin group and AgNP-treated group ($P = 0.54$); whereas the untreated group was found to be statistically significant when compared with both normal ($P = 0.0007$) and AgNP-treated group ($P = 0.0001$). This would suggest that in terms of mechanical properties, AgNP-treated skin showed remarkable similarities to normal skin.

Better stress-strain relationship in AgNP-treated skin

In testing the mechanical properties, we considered the possibility of intersample variation, particularly due to different harvested-skin thickness (which varied from 0.3 to 0.5 mm), which would have a significant impact on the results. In an attempt to control for this, we converted the force-displacement readings to stress and strain, by normalization of data, where the tensile test was indicated by the linear slope in the format of the stress-strain relationship curve (Figure 4). The yielding strength in the stress-strain curve for normal skin, AgNP-treated skin and untreated skin groups was 2.99 ± 0.64 MPa, 2.03 ± 0.42 MPa and 0.57 ± 0.31 MPa, respectively. As in the previous tensile test, there was no statistical difference observed ($P = 0.8501$) between normal skin and AgNP-treated skin. On the other hand, significant difference could be shown between untreated and AgNP group ($P = 0.0026$), and between the untreated and the normal group ($P = 0.0004$). The average elastic modulus calculated from curve was 4.7 ± 1.33 MPa in normal skin; 4.9 ± 1.73MPa in AgNP-treated skin; and 1.2 ± 0.8 MPa in the untreated group.

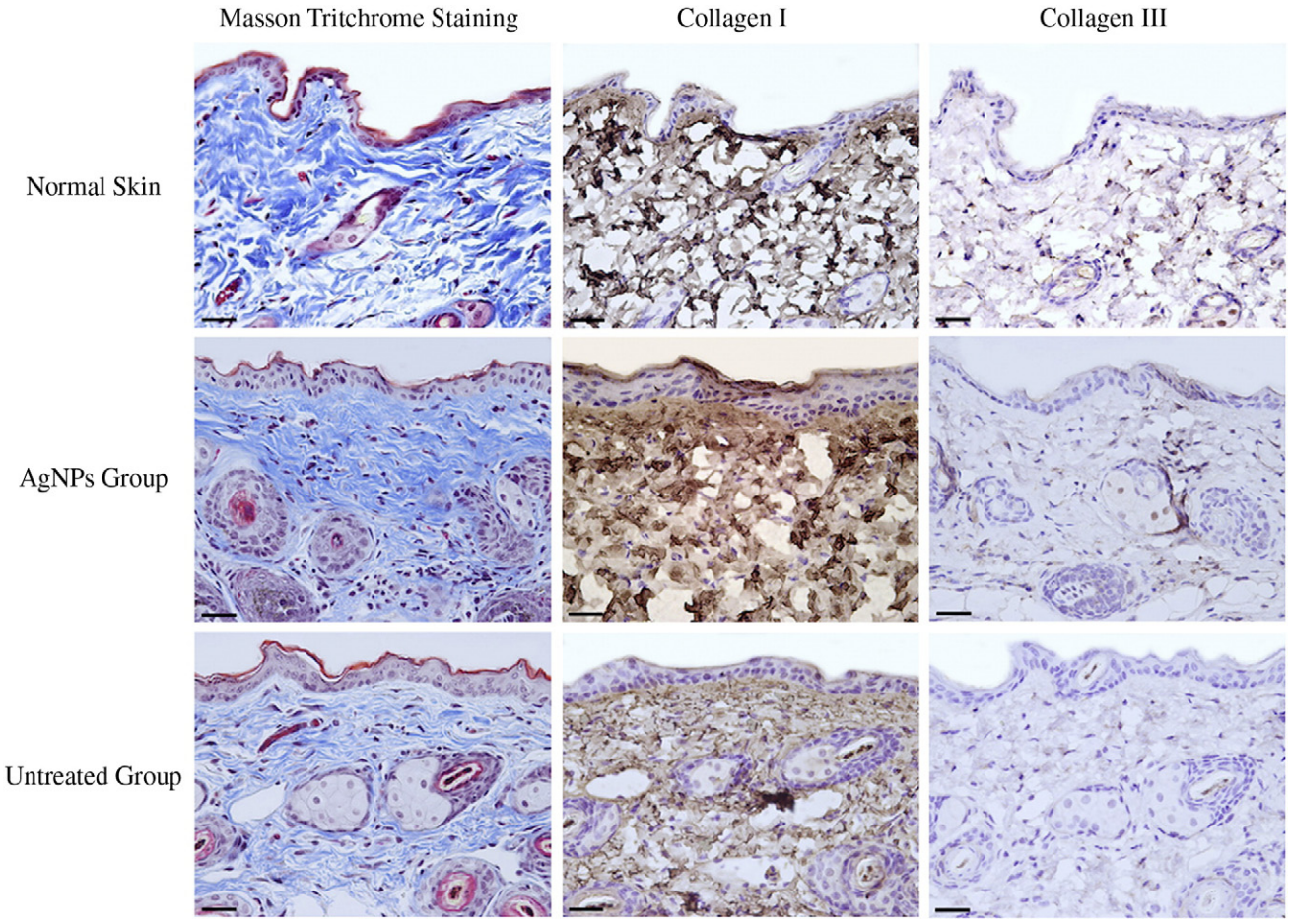

Figure 5. Histological staining of healed skin in each experimental group. Masson Tritchrome staining showed the distribution and density of collagen protein in healed skin in various groups. Under this staining, collagen protein was stained to blue, nuclei were staining to black and background (muscle, cytoplasm and keratin) was stained red. IHC staining showed the expression of collagen type I and type III of healed skin in each group. (Scale bar: 20 um).

Collagen in healed skin treated by AgNPs resembled normal skin

Because of better mechanical properties in AgNP-treated skin, we hypothesized that the collagen laid down in healed tissues would be the most similar to that of normal skin. Hence, cross-sectional morphology and collagen deposition of skin were studied through different staining methods.

Masson tritchrome staining was employed to explore and compare with the overall distribution and density of regenerated collagen in healed skin. Through that process, we observed that normal skin possessed the largest amount of connective tissue/collagen in the dermal layer. For the AgNP group, although there was relatively less collagen, the deposition amount was much more than that seen in the untreated group (Figure 5, left column).

To further dissect out which types of collagen deposition were found in healed tissues, we next explored the differential expression of collagen types I and III, the most abundant types in the extracellular matrix in mammal skin,[12,13] using the IHC. Our results revealed that collagen type I was more abundant in healed skin than was collagen type III. Furthermore, collagen type I expression in AgNP-treated skin were seen to be more than that in the untreated group (Figure 5, middle column). The expression of collagen type III followed a similar trend in the three groups (Figure 5, right column). Furthermore, better spatial distribution could be observed in the AgNP group. In contrast, the untreated sample exhibited a disorganized arrangement with much lower intensity (Figure 5).

To quantify the amount of collagen in the three groups, Hyp detection and protein assay were performed to calculate the ratio of collagen to total protein in healed skin. Results suggested that concentration of total protein in normal skin, AgNP-treated skin and untreated skin was 90.47μg/ml, 74.16μg/ml and 65.50μg/ml, respectively. The corresponding concentrations of collagen were detected as 63.86μg/ml, 47.40μg/ml and 21.78μg/ml, giving protein-to-collagen ratios of 0.71, 0.64 and 0.33, respectively (AgNPs vs. normal: $P = 0.234$; AgNPs vs. untreated group: $P = 0.006$) (Figure 6).

Taken together, it would seem that the better mechanical properties of healed skin treated with AgNPs could be explained by their better resemblance to normal skin and more “normal” deposition of collagen I.

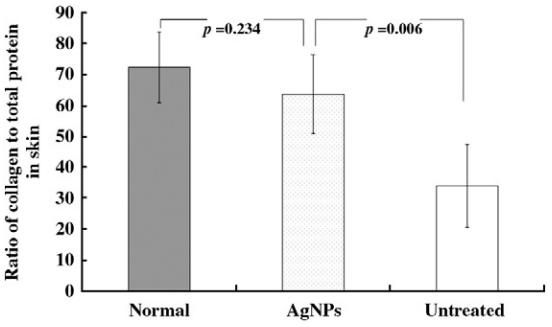

Figure 6. Graph showing the average concentration percentage of collagen in skin. It was calculated to be 72.23%, 63.59% and 33.93% in normal, AgNP-treated and untreated skin, respectively.

Microscopic distribution and morphology of collagen fiber in healed AgNP-treated skin

It is widely known that a major component of skin's tensile property is the alignment and organization of the collagen fibers. Based on the findings of the previous experiments, we next asked if it would be possible that the microscopic distribution and morphology of the collagen fiber of healed skin in each group were different. SEM imaging revealed that the collagen fibrils' arrangement in the normal group and in the AgNP-treated group was regular, and both appeared to be organized. On the other hand, the collagen fibrils were arranged in a relatively chaotic, loose and randomly aligned fibril matrix in the untreated group (Figure 7, *A-C*). Under higher magnification (Figure 7, *D-F*), the fibril detail could be observed clearly. The average diameter of the surface fibrils for each group was measured (n = 100). The average value for normal (D), for AgNP-treated (E) and for the untreated (F) group was 104.3 nm, 78.6 nm and 64.8 nm, respectively. In addition to the fibril diameter, the *D*-periodicity of the collagen fibril was also clearly observed as indicated on normal skin and on AgNP-treated skin (Figure 7, *D*). Morphologically, the fibrils in the untreated sample were apparently different from those of the other two groups with a very irregular fibril outline and lateral fusion with collagen beads along the fibrils.

Furthermore, when we examined the region near the fracture site after specimens in each group were physically ripped, we found that the collagen fibers in normal skin samples and in the AgNP samples demonstrated a more regular and compact pattern, and the untreated sample exhibited a sparse arrangement. Intermingled fibrils were also found in the untreated samples (Figure 8). This further indicated that in healed skin treated by AgNPs, collagen fibers were arranged in a more regular fashion than in the untreated group, which also contributed greatly to the better mechanical properties.

Discussion

From a clinical standpoint, wound healing is a frequent treatment priority. This is especially true for patients who suffer from impaired healing, such as diabetics or those with infected wounds after trauma. Over the years, scientists have sought better methods to promote wound healing. They investigated skin substitutes,[14-17] the fetal wound model,[18-21] modulation of biomolecules[22-25] and oxygen therapy,[26,27] etc., for accelerated and scar-free healing, particularly in treating large and life-threatening wounds.

Our previous studies showed that AgNPs had the potential to promote wound healing through facilitated anti-inflammatory action.[5] Furthermore, it would appear that in the excisional wound model, AgNPs could contribute positively to the process of re-epithelialization and enhanced differentiation of fibroblasts into myofibroblasts, resulting in faster wound contraction during healing.[6] Despite these results, we were not sure whether AgNP-treated skin resulted in potentially better functioning after healing. One way to test this was to look at the mechanical properties of healed skin tissues.

In this study, the strength of skin tissues was investigated by tensile testing. Although tensile tests have been conducted on skin in previous studies, none was performed on AgNP-treated skin.[28-31] Although the yielding load of the AgNP sample was about 60% of that of normal skin in the tensile experiment, this was already significantly better than that of the untreated skin samples. Furthermore, after normalization, the yielding strength was 68%, and the modulus was 104% of that of normal skin. Moreover, it was clear that the loading patterns for the untreated samples were inconsistent. All of the above evidence would suggest that the microstructure of the untreated sample could be different from that of other samples.

From the IHC examinations, more collagen expression was observed in normal and AgNP groups than in the untreated group. It was also seen that the cell distribution in the untreated group was unlike that in the other groups, with random arrangement and cryptogenic structures observed. These findings exactly corresponded to the tensile test result in which normal and AgNP groups showed better strengths than the untreated group showed. The quantitative measurement of collagen content further verified this observation. Hence, it was confirmed that skin's tensile properties depended on the level of collagen expression, especially type I collagen, and somehow related to the way cells and other biomolecules were arranged during the healing process.

From the cosmetic appearance and histological examination, it was not surprising to record similar tensile properties between the normal and AgNP group. The tensile test results could be explained objectively by visualizing their microstructures, particularly the collagen network and features. It is generally conceived that skin strength correlates directly with the overall organization, content and physical properties of the collagen fibril network.[32] The basic unit of the structural hierarchy of collagen tissue is a triple helix collagen molecule of approximately 300 nm.[33] The collagen molecules self-assemble axially in a regular pattern to form a *D*-periodic cross-striated fibril.[33] The fibrils are then bundled together into a collagen fiber. In this study, although the molecular level of collagen was not examined in detail, the *D*-periodicity of fibrils can be clearly seen on SEM in normal skin, as well as in AgNP-treated healed skin. This is in contrast to the less prominent striated pattern in untreated skins and likely to be due to the disorganized assembly of the collagen molecules.

Collagen fibers fail under stress via three steps of deformation: collagen molecular deformation, fibril deformation and

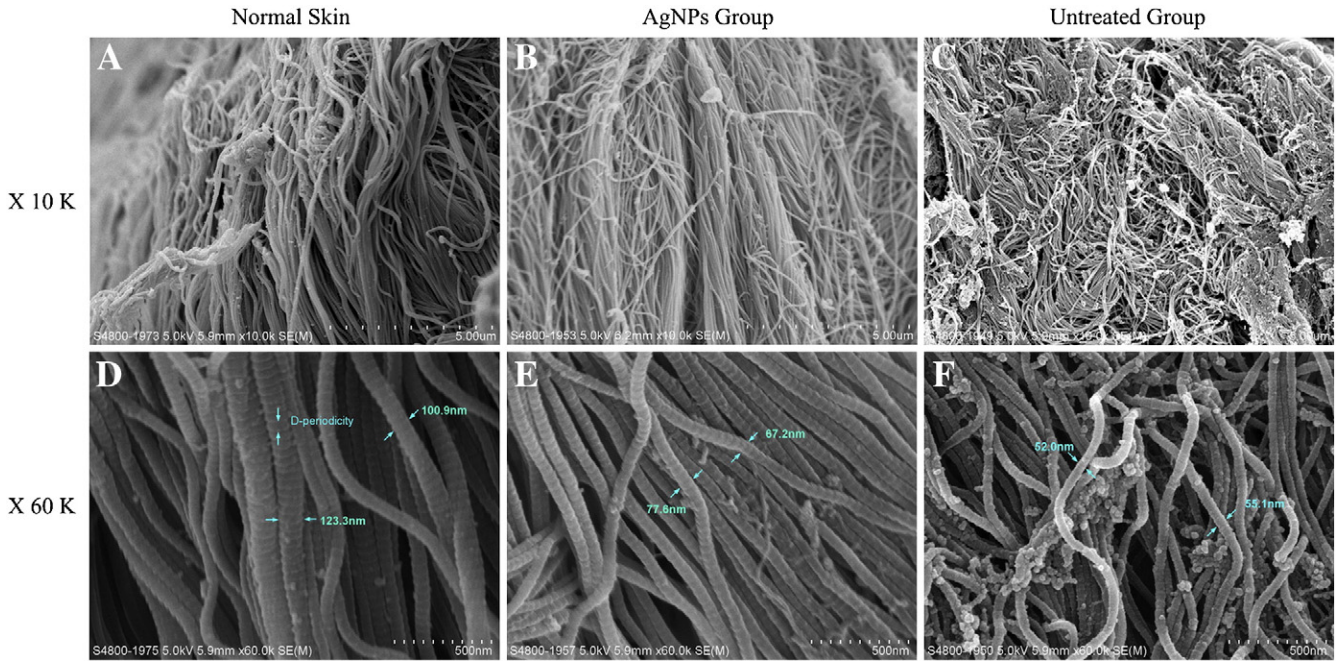

Figure 7. Collagen fibrils matrices were shown in the SEM imaging. In lower magnification (x 10,000), it was observed that the fibrils arrangement between the normal **(A)** and AgNP-treated groups **(B)** were very similar in comparison with that of the untreated group **(C)**. The normal and AgNP-treated groups had much more organized structure in contrast to the loose and randomly aligned fibril matrix of the untreated sample. In higher magnification (x 60,000), the average diameter of the surface fibrils for each group was measured. In addition, the *D*-periodicity of the collagen fibril was also clearly observed as indicated on normal skin **(D)**. Fibrils in untreated sample were apparently different from those of the other groups with very irregular fibril outline and lateral fusion with collagen beads along the fibrils.

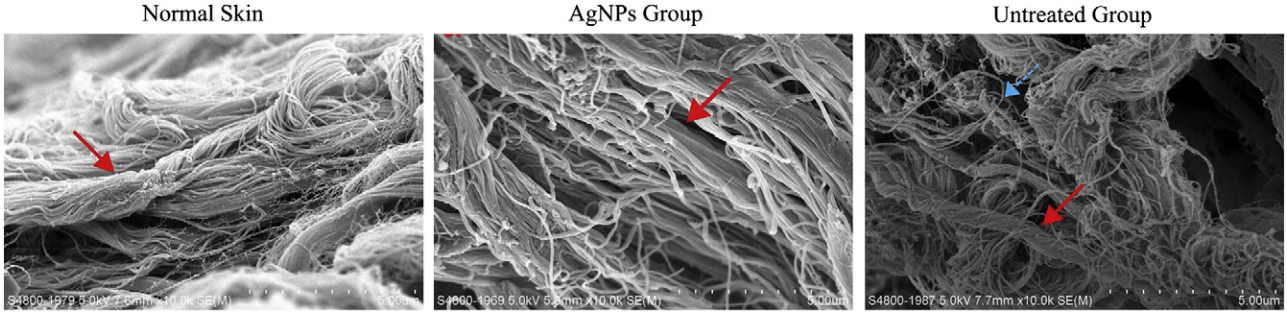

Figure 8. SEM pictures showing region near the fracture site (x 10,000). Although collagen fibers (indicated with red arrows) were observed in all samples, the normal skin sample and the AgNP sample demonstrated a more regular and compact pattern, and the untreated sample exhibited a sparse arrangement. Intermingled fibrils (indicated with blue dotted arrow) were also found on the untreated samples.

tissue deformation.[34] As observed in this study, the fibrils in untreated samples were aligned in an irregular manner, which implied that the length of fibrils varied significantly within a distance. When tensile stress was applied, the fibrils experienced deformation at different moments, and the total number of fibrils resisting the tensile force was reduced. Eventually fibrils failed in small bundles rather than in a large healthy collagen fiber. The benefit of fibrillar arrangement in collagen fiber was thus lost. This explained why the untreated group had much lower resistance to tensile loading than the other groups had.

The fluctuation in the load-displacement curve of the untreated samples can also be explained with the above theory. Yielding was recorded whenever bundles of fibrils were torn, and that was graphically represented by the multiple peaks on the curve. Unlike the untreated samples, collagen fibrils in normal and in AgNP-treated skins broke almost simultaneously due to their homogenous arrangement, thus resulting in smoothly loading curves with a single peak. In addition, the average diameter of collagen fibril in untreated group was only 82% and 62% of that of AgNP- and normal-skin fibril, respectively. This contributes directly to the low strength of the untreated samples.

Apart from evaluation of the tensile test result, a “spaghetti and lentils” appearance was observed in the SEM pictures. In normal and AgNP samples, very nicely arranged spaghetti-

like collagen fibers were seen, whereas aggregated and randomly oriented fibers were found in untreated samples. “Lentils”-like collagen beads were also observed to attach to the “spaghetti” in untreated samples. These findings can be attributed to the uncontrolled deposition of collagen during the natural wound-healing process. On the other hand, the characteristics of collagen fibers in the AgNP group were essentially different and greatly resembled those found in normal skin. This was concrete evidence that AgNPs modulate collagen deposition in wound healing, and this also explained why AgNP-treated wounds demonstrated fetal wound healing rather than forming scars.

This study investigated the tensile property of the healed skin tissue treated with AgNPs in an excisional wound model. The findings further provided evidence that AgNPs not only had a beneficial effect on acceleration of the wound-healing process, but also improved the tensile properties of the repaired skin, with a close resemblance to normal skin. We postulate that this effect is achieved by the ability of AgNPs to regulate the deposition of collagen and inhibiting uncontrolled growth of collagen, as well as directing proper collagen matrix alignment and spatial arrangement. This may be achieved through a regulated differentiation of fibroblasts and collagen production.[6] However, the molecular pathway for which AgNPs affect collagen regeneration is yet to be investigated. To conclude, this study provides additional insight into the role of AgNPs in the process of wound healing and leads clinicians one step closer to the clinical application of these fascinating biomaterials.

References

1. Midwood KS, Williams LV, Schwarzbauer JE. Tissue repair and the dynamics of the extracellular matrix. Int J Biochem Cell Biol 2004;36:1031-7.
2. Singer AJ, Clark RA. Cutaneous wound healing. N Engl J Med 1999;341:738-46.
3. Fratzl P, Misof K, Zizak I, Rapp G, Amenitsch H, Bernstorff S. Fibrillar structure and mechanical properties of collagen. J Struct Biol 1998;122:119-22.
4. Lee PY, Chesnoy S, Huang L. Electroporatic delivery of TGF-beta1 gene works synergistically with electric therapy to enhance diabetic wound healing in db/db mice. J Invest Dermatol 2004;123:791-8.
5. Tian J, Wong KK, Ho CM, Lok CN, Yu WY, Che CM, et al. Topical delivery of silver nanoparticles promotes wound healing. ChemMedChem 2007;2:129-36.
6. Liu X, Lee PY, Ho CM, Lui VC, Chen Y, Che CM, et al. Silver nanoparticles mediate differential responses in keratinocytes and fibroblasts during skin wound healing. ChemMedChem 2010;5:468-75.
7. Martin P. Wound healing: aiming for perfect skin regeneration. Science 1997;276:75-81.
8. Saap LJ, Falanga V. Debridement performance index and its correlation with complete closure of diabetic foot ulcers. Wound Repair Regen 2002;10:354-9.
9. Myers SR, Partha VN, Soranzo C, Price RD, Navsaria HA. Hyalomatrix: a temporary epidermal barrier, hyaluronan delivery, and neodermis induction system for keratinocyte stem cell therapy. Tissue Eng 2007;13:2733-41.
10. Medugorac I. Myocardial collagen in different forms of heart hypertrophy in the rat. Res Exp Med (Berl) 1980;177:201-11.
11. Lopes JD, Gomes RA, Hial V, Lopes IC, Reis MA, Teixeira Vde P. Correlations between the collagen content of the human left ventricular myocardium, measured by biochemical and morphometric methods. Arq Bras Cardiol 2002;79:10-9.
12. Orgel JP, Miller A, Irving TC, Fischetti RF, Hammersley AP, Wess TJ. The in situ supermolecular structure of type I collagen. Structure 2001;9:1061-9.
13. Puxkandl R, Zizak I, Paris O, Keckes J, Tesch W, Bernstorff S, et al. Viscoelastic properties of collagen: Synchrotron radiation investigations and structural model. Philos Trans R Soc Lond B Biol Sci 2002;357:191-7.
14. Bello YM, Falabella AF, Eaglstein WH. Tissue-engineered skin. Current status in wound healing. Am J Clin Dermatol 2001;2:305-13.
15. Nakagawa H, Akita S, Fukui M, Fujii T, Akino K. Human mesenchymal stem cells successfully improve skin-substitute wound healing. Br J Dermatol 2005;153:29-36.
16. DeCarbo WT. Special segment: soft tissue matrices–Apligraf bilayered skin substitute to augment healing of chronic wounds in diabetic patients. Foot Ankle Spec 2009;2:299-302.
17. Burke JF, Yannas IV, Quinby WCJ, Bondoc CC, Jung WK. Successful use of a physiologically acceptable artificial skin in the treatment of extensive burn injury. Ann Surg 1981;194:413-28.
18. Lorenz HP, Whitby DJ, Longaker MT, Adzick NS. Fetal wound healing. The ontogeny of scar formation in the non-human primate. Ann Surg 1993;217:391-6.
19. Bullard KM, Cass DL, Banda MJ, Adzick NS. Transforming growth factor beta-1 decreases interstitial collagenase in healing human fetal skin. J Pediatr Surg 1997;32:1023-7.
20. Adzick NS, Lorenz HP. Cells, matrix, growth factors, and the surgeon. The biology of scarless fetal wound repair. Ann Surg 1994;220:10-8.
21. Liechty KW, Adzick NS, Crombleholme TM. Diminished INTERLEUKIN 6 (IL-6) production during scarless human fetal wound repair. Cytokine 2000;12:671-6.
22. Fu X, Li X, Cheng B, Chen W, Sheng Z. Engineered growth factors and cutaneous wound healing: success and possible questions in the past 10 years. Wound Repair Regen 2005;13:122-30.
23. Malinda KM, Sidhu GS, Mani H, Banaudha K, Maheshwari RK, Goldstein AL, et al. Thymosin beta 4 accelerates wound healing. J Invest Dermatol 1999;113:364-8.
24. Montesano R, Orci L. Transforming growth factor beta stimulates collagen-matrix contraction by fibroblasts: implications for wound healing. Proc Natl Acad Sci U S A 1988;85:4894-7.
25. Werner S, Grose R. Regulation of wound healing by growth factors and cytokines. Physiol Rev 2003;83:835-70.
26. Knighton DR, Silver IA, Hunt TK. Regulation of wound-healing angiogenesis-effect of oxygen gradients and inspired oxygen concentration. Surgery 1981;90:262-70.
27. Chandan KS, Savita K, Gayle G, Debasis B, Manashi B, Sashwati R. Oxygen, oxidants, and antioxidants in wound healing. Ann N Y Acad Sci 2002;957:239-49.
28. Lu WW, Ip WY, Jing WM, Holmes AD, Chow SP. Biomechanical properties of thin skin flap after basic fibroblast growth factor (bFGF) administration. Br J Plast Surg 2000;53:225-9.
29. Danielson KG, Baribault H, Holmes DF, Graham H, Kadler KE, Iozzo RV. Targeted disruption of decorin leads to abnormal collagen fibril morphology and skin fragility. J Cell Biol 1997;136:729-43.
30. Smith MJ, Haltom JD, Gainor BJ. Effects of anticoagulation on wound healing using a tensile test. Orthopedics 2008;31:373-7.
31. Chakravarti S, Magnuson T, Lass JH, Jepsen KJ, LaMantia C, Carroll H. Lumican regulates collagen fibril assembly: skin fragility and corneal opacity in the absence of lumican. J Cell Biol 1998;141:1277-86.
32. Dombi GW, Haut RC, Sullivan WG. Correlation of high-speed tensile strength with collagen content in control and lathyritic rat skin. J Surg Res 1993;54:21-8.
33. Kadler KE, Holmes DF, Trotter JA, Chapman JA. Collagen fibril formation. Biochem J 1996;316(Pt 1):1-11.
34. Sasaki N, Odajima S. Elongation mechanism of collagen fibrils and force-strain relations of tendon at each level of structural hierarchy. J Biomechanic 1996;29:1131-6.